Accepted Manuscript

Ethane clathrates using different water-ethane models: Molecular dynamics

G. Torres-García, D.P. Luis, G. Odriozola, J. López-Lemus

PII: S0378-4371(17)30908-1
DOI: https://doi.org/10.1016/j.physa.2017.09.016
Reference: PHYSA 18621

To appear in: *Physica A*

Received date : 3 September 2017

Please cite this article as: G. Torres-García, D.P. Luis, G. Odriozola, J. López-Lemus, Ethane clathrates using different water-ethane models: Molecular dynamics, *Physica A* (2017), https://doi.org/10.1016/j.physa.2017.09.016

HIGHLIGHTS

The performance of different water models in ethane clathrates was analysed by molecular dynamics simulations. The study was carried out inside of the temperature regime where a stable-unstable transition takes place.

None of the considered water models was able to reproduce the transition temperature by using the standard Lorentz-Berthelot combining rules.

The current manuscript shows that a slight modification on combining rules allows us to approach to the experimental temperature. By modifying both cross terms, the intensity of attraction and the average size of atoms, the decomposition of ethane clathrates was observed.

Such process was evidenced by monitoring the coordination number, hydrogen bonds, radial distribution functions, mean force potential and the mean square displacement. Based on these results we mentioned that the entropic effects are also important as enthalpic ones.

Ethane clathrates using different water-ethane models: molecular dynamics

G. Torres-García[a], D.P. Luis[b], G. Odriozola[c] and J. López-Lemus[a1]

[a]Facultad de Ciencias, Universidad Autónoma del Estado de México, Toluca, CP 50295, México.
[b]CONACYT Research Fellow-Centro de Ingeniería y Desarrollo Industrial, Querétaro, CP 76125, México.
[c]Área de Física de Procesos Irreversibles, División de Ciencias Básicas e Ingeniería, Universidad Autónoma Metropolitana-Azcapotzalco, D.F., CP 02200, México.

Abstract

Ethane clathrates are studied in a temperature window where the stable-unstable transition takes place by means of molecular dynamics simulations in an isothermal–isobaric ensemble. For this purpose a temperature range [200–440] K and a pressure of 2 MPa are considered. Firstly, structural analysis of the ethane clathrates is carried out at a fixed temperature of 200 K, where clathrates are stable for all considered water models. Here, it is found that structural properties of all stable clathrates do not strongly depend on the water model. As a next step, temperature is increased upon the clathrate turns unstable. This decomposition temperature is found by monitoring coordination numbers, total number of hydrogen-bonds, potential energy, potential of mean force and mean-square displacements. All properties consistently point out to the same temperature at which the stable–unstable transition takes place for each water model. As a part of our results, we notice that by using the standard Lorentz-Berthelot combining rules, the obtained temperature at which the clathrate becomes unstable is higher than the experimental reference value for all used water models. However, we have found that a reasonable way to approach the experimental-decomposition temperature is by including a re-scaling factor in the combining rules in such a way that both methyl–oxygen size and interaction energy turned out decreased. Our data indicates that the decomposition temperature is sensitive to both parameters.

keywords: Ethane clathrates, combining rules, molecular dynamics

[1]jllemus@uaemex.mx

1 Introduction

Natural gas hydrates are crystalline nonstoichiometric compounds usually formed at low temperatures and high pressures. These crystalline arrangements are compounded by water and a nonpolar molecule. Most of the gas hydrates are classified into three structural groups, sI, sII, and sH [1, 2, 3, 4]. Typically, the type of the crystalline structure is determined by the guest-molecule size. Structure sI is observed for methane, ethane, carbon dioxide and hydrogen sulfide. It consists of two pentagonal dodecahedron (5^{12}) cavities and six tetrakaidecahedron constituted by twelve pentagonal and two hexagonal faces ($5^{12}6^2$) [1]. Structures sII usually contain a small guest molecule, for example, hydrogen, oxygen, propane or nitrogen. This type of structure is formed by 16 dodecahedral 5^{12} cages and 8 hexakaidecahedral $5^{12}6^4$ cages [2]. The sH clathrate is formed with larger molecules either bromocyclopentane (BrCP) or bromocyclohexane (BrCH) [3, 5], as an example. In contrast with the previous structures, the sH clathrates consist of three types of cavities. It contains three 5^{12} cages, an icosahedron $5^{12}6^8$ cage, and two irregular dodecahedron cavities denoted as $4^35^66^3$, which means that it has three square faces, six pentagonal faces and three hexagonal faces [3, 4].

The study of gas hydrates is an interesting aim because the vast reserves of natural gas hydrates represent an important energy source. The recovery of hydrocarbon from this source is, however, a complex challenge due to the risks of an environmental accident. There are other economic issues related to transportation of natural gas along the extracting line. Clathrates can appear inside the pipelines under suitable thermodynamic conditions which can impede the normal flow. Traditionally, some type of alcohol (*e.g.* methanol) is used to decrease the formation temperature avoiding the clathrate blockage [6]. Other strategies involve a kinetic inhibitor [7].

The growing of clathrates hydrates has been widely analysed [8, 9, 10, 11], however, the decomposition of this same kind of crystalline compounds has not been explored in the same way. Bishnoi and Natarajan [12] have pointed out that the hydrate decomposition is a sequence of structural arrangements and breakages, as well as the gas desorption processes. Baez and Clancy [10] analysed methane clathrates by molecular simulations showing that the dissociation is a stochastic process. There are interesting contributions where the clathrates dissociation has been studied by applying an external perturbation such as the incidence of electric fields [11, 13, 14]. In general, simple hydrates as methane-clathrates have attracted more attention than ethane-clathrates. Nonetheless, there are important contributions regarding the analysis of ethane clathrates and their mixtures with other small carbon molecules [9, 11, 15, 16, 17]. For example, Morita *et al.* [18] have analysed experimentally the stability of ethane hydrates, and among theirs findings, they report that the ethane molecules occupy all cavities in the sI structure. Naseh *et al.* [19] performed experiments in order to study the mass transfer phenomenon of ethane during hydrate formation. Tanaka

studied the thermodynamic stability of non-spherical guests such as ethane and propane by using the generalized van der Waals and Platteeuw theory. In that same work the occupation rates were also estimated by means of grand canonical Monte Carlo simulations [20].

To analyse the decomposition process of gas clathrates from a molecular simulation framework, is required a water model capable of matching the estimated data by molecular simulation to the experimental-decomposition temperature. To the best of our knowledge, this kind of analysis has not been performed on ethane clathrates. The stable structure of the ethane clathrates at T=200 K and 2 MPa, can be reproduced by using more than one water model since the results from molecular simulations seem to be independent of the water model used. However, the choice of water and ethane models becomes an important topic for obtaining the best performance in a stable-unstable transition (around T=285 K), especially, when the dissociation of crystalline compound is studied using different methods, for instance, by adding an alcohol or applying an external perturbation. In fact, our main interest lies on this last topic, but first we need a good enough model for both water and ethane molecules.

The aim of this work is to determine which water model reproduces the transition temperature of ethane clathrates, comparing the performance of both united atom and all-atoms models for the ethane molecule, and verifying if the standard Lorentz–Berthelot combining rules are enough to obtain good results. We first compared the structure of ethane clathrates by using different water models under stable thermodynamic conditions. This is carried out by means of molecular simulations in an isothermal–isobaric ensemble. Then, we examined the temperature at which the system destabilize and compare this value with the experimental one. Structural and dynamic properties are calculated for capturing the beginning of a loss of stability of crystalline compounds. The rest of the work is organized as follows: the simulation details are reported in section 2. Whereas in section 3, the results are shown and discussed. Finally, conclusions are given in section 4.

2 Methodology and simulation details

Different water models were considered to determine which one is the most convenient model to reproduce the transition from a stable to unstable state of the ethane clathrate by increasing temperature [4]. The used water models are the following: the models of three sites SPC [21] and SPC/E [22], the models of four sites TIP4P [23], TIP4P/2005 [24], TIP4P/ICE [25], TIP4Q [26] and a model of five sites TIP5P [27]. The NERD ethane model was used in most of the simulations [28], which is constituted by two pseudoatoms (two methyl groups, $2CH_3$) bonded each other. Both pseudoatoms contribute to the energy through the Lennard-Jones potential. In addition, molecular simulations using the

OPLS/AA [29] force field were performed in order to compare the contribution of the explicit hydrogens. Most of the simulations were performed by using the standard Lorentz [30] and Berthelot [31] combining rules for estimating the cross interaction between different species. In addition, two series of simulations were carried out only for the SPC water model including an empirical correction factor $\chi < 1$ in the aforementioned combining rules. In one case, the χ factor was included just in the Berthelot rule and in other case, the same factor was included in both geometrical and arithmetic rules for ϵ_{ij} and σ_{ij}, respectively. These last two combining rules can be read as

$$\begin{aligned} \sigma_{ij} &= \frac{(\sigma_{ii} + \sigma_{jj})}{2} \\ \epsilon_{ij} &= \chi\sqrt{\epsilon_{ii}\epsilon_{jj}}, \end{aligned} \tag{1}$$

$$\begin{aligned} \sigma_{ij} &= \frac{\chi(\sigma_{ii} + \sigma_{jj})}{2} \\ \epsilon_{ij} &= \chi\sqrt{\epsilon_{ii}\epsilon_{jj}}, \end{aligned} \tag{2}$$

where σ_{ii} and ϵ_{ii} are the diameter and the attraction well depth between sites of the i species, respectively. χ equals unity in case of the original combining rules. The standard Lorentz–Berthelot combining rules have been widely used for estimating the unlike dispersion interactions in different type of systems. In some works the effect of these combining rules on the thermodynamic properties of different types of mixtures has been reported [32, 33, 34]. In some instances only one rule has been modified, e.g. Díaz *et al.* [35] have modified the combining rule ϵ_{ij} to tune the miscibility of the two simple fluids. In another contribution, this type of modification was used for analysing the excess chemical potential of methane in an aqueous electrolyte solution incorporating NaCl [36]. Despite the relevancy of this issue there is only a few contributions where the convenience of considering modified combining rules in clathrates hydrates is analysed [37, 38, 39, 40]. In some of them only one rule is modified [37, 38], and in other instances both rules were modified [39, 40].

Molecular dynamic simulations are performed in an isothermal–isobaric ensemble. The free software Gromacs/4.5.5 [41, 42, 43, 44] is used to carry out the simulations. The leap-frog algorithm is employed to integrate the equations of motion. Periodic boundary conditions and the minimum image convention were considered along the three spatial directions. The cut-off distance for the Lennard-Jones potential and for the real space contribution of the Coulomb potential is set at 1.2 nm. The long range Coulomb interaction is handled by the Particle Mesh Ewald method (PME) [45]. The time step in all our simulations is Δt=1 fs and all the runs are carried out until 20 ns. The LINear Constraint Solver (LINCS) [46] method is used to maintain constant the bond distances in each molecule. The Berendsen

barostat [47] and the Nosé-Hoover chain thermostats with 0.4 ps as time constants [48] are used to set pressure and temperature, respectively. A comparison between the Berendsen and Parrinello-Rahman [49] barostats was carried out in order to dispose of suitable adjustment parameters. As a result, no significant differences were observed since both barostats efficiently maintained the system under a constant pressure.

The initial configuration for ethane clathrates is taken from the experimental evidence supplied by McMullan and Jeffrey [50]. Although, the original array was settled for ethylene oxide hydrates, it provides the correct location of the water oxygens. In addition, the location of the guest molecules inside the cages is also provided. From this information it is easy to build the ethane molecule using two methyl pseudoatoms. The unit cell is constituted by 46 water molecules and 8 ethane molecules with dimensions $L_x = L_y = L_z = 12.03$ Å and replicated $2 \times 2 \times 2$ times to yield the simulation cell with dimensions $L_x = L_y = L_z = 24.06$ Å. This simulation box contains 368 water molecules and 64 ethane molecules. It is worth noticing the sI structure is adequate here since a typical guest molecule could have diameters between 4.2 and 6$\mathring{A}$ as the ethane case, which has an effective diameter and length of 3.988$\mathring{A}$ and 4.755$\mathring{A}$ [4, 51, 52], respectively. For building the initial configuration, protons are added according to the Bernal–Fowler rules [53] where each water molecule is oriented in such a way that its two hydrogen atoms are directed approximately toward two of the four surrounding oxygen atoms and only one hydrogen atom is located on each oxygen-oxygen linkage, followed by a short NPT simulation at a low temperature (50 ps, T=50 K, P=2 MPa). This procedure leads to a low free energy structure for each water model. Furthermore, the procedure allows us to obtain a null dipole moment of the simulation cell. Once low free energy initial configurations are built, the production runs are performed in a NPT ensemble at P=2 MPa in a temperature range [200–440] K. We are fixing pressure to 2 MPa since the experimental decomposition temperature was estimated for this value, among others [4].

From the obtained trajectories we have performed a structural and dynamical analysis. The coordination number, $n(d)$, between ethane and water molecules was calculated through the radial distribution function (RDF) $g(r)$ [54] as follows

$$n(d) = 4\pi\rho \int_0^d r^2 g(r) dr \tag{3}$$

where ρ is the density number of the water molecules, and distance d is taken at the end of the first coordination shell. The Potential of Mean Force (PMF), W(r), which is defined as the free energy required to put together a pair of atoms at a distance r bringing them from infinity, is estimated as follows

$$W(r) = -k_B T ln(g(r)) \tag{4}$$

k_B is the Boltzmann constant and T is a given temperature.

The hydrogen-bonds are also estimated between all available donors and acceptors. A geometrical criterion is employed to determine possible H-bonds, the distance between donor-acceptor was settled as $r \leq r_{HB} = 0.35$ nm, which corresponds to the first minimum of the hydrogen-oxygen $g(r)$ of the water model. The criterion also considers the angle between the O–O axis and the O–H bonds to be lower than 30°. Further details are reported elsewhere (Luzar and Chandler [55]). Finally, the mean-square displacement (MSD) is calculated as a function of time. This quantity is linked to the diffusion coefficient, D, through the Einstein relationship [56] as follows

$$< [r(t) - r(0)]^2 >= 6Dt \tag{5}$$

where $r(t)$ is the molecule position at time t, $r(0)$ is the position at a reference time, and $< \cdots >$ stands for the average over different reference times.

3 Results and discussion

Before performing the destabilization analysis, we first focus on the structural properties of clathrates at low temperatures, where the crystalline compound is stable for all water models. We open this section by comparing the radial distribution functions for methyl–methyl (me–me) and methyl–oxygen (me–O) sites of all considered water models. The radial distribution functions for me–me and me–O were estimated at T=200 K and P=2 MPa. This temperature is far from the experimental critical temperature where the stable-unstable transition takes place, which at P=2 MPa is around T=285 K [4]. The standard Lorentz-Berthelot combining rules ($\chi = 1$) were used in these simulations.

Figure 1 shows the me–me RDF's for all the considered water models at the same low temperature T=200 K. The crystal-like structure is evident from the structured RDFs, which is built from localized methyl groups. As can be seen, all water models yield practically the same curves, pointing out a robust ethane clathrate hydrate structure which is insensitive to the employed model. In fact, all water models produce a stable structure at these thermodynamic conditions. The average separation between first neighbours of pseudoatoms me–me is, for all cases, around 0.61 nm. This distance can be compared to that one obtained for methane clathrates, which is 0.65 nm [57]. This small difference can be simply attributed to the fact the only site of methane molecule coincides with its geometric center but in the case of ethane, the geometric center do not coincides with the position of the methyl pseudo-atom.

Figure 2 shows the me–O RDF's in correspondence to Figure 1, that is to say, for the same simulations performed at T=200 K. In all cases, the me–O RDFs have a first peak at a

distance around 0.38 nm. Again, this first peak distance can be compared with that one obtained for methane clathrates. This distance is 0.39 nm [57], confirming that the structure of this kind of clathrates is not sensitive to the size of the guest molecule. As in the previous case, the smaller me–O distance can be simply attributed to the guest geometry. On the other hand, our value compares well with the distance reported by Mancera *et al.* for T=279 K, 0.39 nm [58]. In that case the SPC water model and the NVE ensemble were employed. Figure 3 shows a snapshot of the ethane clathrate with the SPC water model. In order to analyse a possible modification on spatial arrangement due to the periodic boundary conditions, a series of simulations were performed using a $3 \times 3 \times 3$ simulation cell (not shown). Basically, there are not significant differences among the resulting curves.

A direct way to detect the destabilization of the structure is by means of the water coordination number of ethane molecules. This quantity is quite sensitive to the system structure. There are 24 oxygen atoms surrounding a carbon for the ethane clathrate structure according to the information supplied by Sloan and Koh [4]. This number is plotted as a function of temperature in figure 4a. Again, the pressure is fixed at 2 Mpa for all considered water models. The temperature was increased upon finding a sharp decrease of the coordination number, that is, a destabilization of the clathrate structure (this destabilization is confirmed by a structural analysis, and it strongly correlates with abrupt potential energy changes). This sharp drop of the coordination number can vary from 25 to 5 oxygen atoms for both SPC/E and TIP4P water models, and from 25 to 15 oxygen atoms for TIP4P/2005.

As shown in figure 4a, the temperature at which the destabilization occurs is far from the experimental evidence. This figure allows to observe a strong dependence on the employed water model. This fact contrasts with the structural analysis performed at 200 K, where different water models lead to practically the same structure. Figure 4a also shows that the SPC, SPC/E, and TIP4P models reach the smallest decomposition temperatures. These models lead to decomposition temperatures inside the range [320–360] K. They all are, however, larger than the experimental value of 285 K. Indeed, the closest decomposition temperature to the experimental one, is obtained for the SPC water model, i.e. 320 K. Actually, the SPC model has been used in previous works regarding methane and carbon dioxide hydrates [59]. The other water models lead to much larger decomposition temperatures. As an extreme case, the TIP4P/ICE water model yields the most stable system. Hence, none of the considered water models is able to reproduce the experimental temperature using the standard combining rules(385 K) [4, 9]. This is despite the fact that the models used here for water [21, 22, 24] and ethane [28, 29] molecules yield reasonable results as pure compounds. In fact, experimental bulk and interfacial properties have been reproduced for both type of molecules. Indeed, both models were not built especially to mimic clathrates and may represent a source of deviation, in particular, cross interaction could contribute to the mismatch of the experimental decomposition. At relative low temperature (T=250 K) the

crystalline compound remains formed by using either SPC or TIP4P/ICE water model this fact indicates that both water models work very well at this thermodynamics state, however as soon as the temperature is increased the destabilization of the system is captured at different temperatures depending on the water model. As it is well known the stability of the crystalline compound depends on the guest [4]. So, when the thermal contribution becomes as important as the molecular interaction then the hydrogen-bonds turn out weakened, in this way the stability of the system lies on the cross interaction, and tuning this interaction can be possible to reproduce the experimental temperature where the stable-unstable transition takes place. We observe that our results did not change significantly when simulations up to 50 ns were performed. This can be important since the clathrate structure can persist in a metastable state before decomposing specially when the system does not have any interphases. Nonetheless, the relatively small simulation cells, that we are employing favor thermodynamic fluctuations which makes it easier that the system can escape from local free energy minima.

With the aim of approaching the experimental results, we consider two modifications on the combination rules. Firstly we tried only changing the Berthelot rule (by rescaling the energetic scale). For this purpose a χ parameter for the methyl-oxygen interaction was included. A second test was then implemented by rescaling energy and distance. These modifications were tested for the SPC water model. The effect of varying χ on the ethane coordination number is shown in figure 4b. Here we are showing only the reference case (with the original rules, $\chi = 1$) and the two cases capable of reproducing the experimental value. These cases correspond to $\chi = 0.035$ when only the energy scale was rescaled, and to $\chi = 0.83$ when both combining rules are rescaled by this factor. The decomposition temperature is much more sensitive to a decrease of the interaction distance (molecular size) than to a reduction of the energetic scale. This implies that the clathrate stability is much more dependent on the size of the guest than on its ability to strongly interact with the water cage. In other words, the guest stabilizes the clathrate by decreasing the water degrees of freedom, *i. e.*, by entropic reasons. In fact, a value of $\chi = 0.035$ cannot be easily justified while $\chi = 0.83$ seems much more reasonable. It is worth mentioning that combining rules are of an empiric nature. Thus, it should not come as a surprise that for certain molecular pairs, such as a strong hydrogen-bonding dipole and a non-polar molecule, the rule leads to not so good results. Indeed, proposing modifications in combining rules is not a rare practice [37, 38, 60]. Similar results are expected for the other water models, for instance, for TIP4P water model the obtained parameter was $\chi = 0.62$.

Another possible way to detect the destabilization of the clathrate structure is by means of the total number of hydrogen-bonds. We have included this number as a function of temperature in figure 5. This figure shows the same cases presented in figure 4. Here, symbols and colors are in correspondence with this figure. As expected, for all cases the number

of hydrogen-bonds decreases as increasing temperature. Although this decrease is not very pronounced in the temperature window, where the clathrates are stable. Once the clathrates decompose to form a liquid-like mixture there appears to be a sharp decrease in the number of hydrogen bonds. These drops are strongly correlated with the drops observed for the coordination number of ethane molecules. Thus, both quantities are good global parameters for detecting the decomposition of the clathrate structure. Conclusions from these data are, thus, identical to those already given in previous paragraphs. In the sense that the modification on both parameters of combining rules allow us to capture the right temperature where the stable-unstable transition of crystalline compound is observed. The numerical value for χ is the same as the coordination number case, see fig. 4.

Given a temperature at which the clathrate begins to lose stability, it is possible to analyse the structural changes based on energetic terms. The structural changes suffered by the crystalline compound are related to the free-energy height which is a barrier that the system must overcome to reach the stable phase. This is consistent with the fact the dissociation is a stochastic process [10]. In this case, the overall lowering of free energy is accompanied with an increase of the potential energy (the price is over-payed with an entropy gain). This potential energy gain is abrupt and easy to detect and points out that a structural change has taken place [38]. This is shown in figure 6a for some selected cases. These are for the SPC water at 285 K, for $\chi = 1$, $\chi = 0.035$ (only affecting the energy scale) and $\chi = 0.83$ (affecting both, energy and distance). We have also included the case for $\chi = 1$ and T=330 K. An invariant potential energy was observed in the low temperature case for $\chi = 1$. This simply means that no decomposition of the clathrate was observed when standard Lorentz-Berthelot combining rules were used at T=285 K. For the cases where the combining rules were affected, they show a dramatic increase of the potential energy denoting a structural change of the system. For the case where only ϵ_{ij} was modified the energy gap is of 2000 KJ/mol. In the other case, the increase is close to 2500 KJ/mol. Note that the potential energy of the clathrate structure is similar for cases with $\chi = 1$ and $\chi = 0.83$, but computer simulations with $\chi = 0.035$ lead to a larger potential energy. This confirms that cases with $\chi = 0.035$ cannot be easily supported. We are also including the case for $\chi = 1$ at T=330 K. This last situation also leads to destabilization and to an increase of potential energy close to 2500 KJ/mol. A significant change on potential energy was observed only when the χ parameter was included in the cross interactions at T=285 K. Indicating that a stable-unstable transition takes places on the crystalline compounds.

We have performed computer simulations by using the force field OPLS/AA [29] for ethane molecules, which explicitly considers all hydrogen atoms. This was done to explore the possibility of detecting a shift of the decomposition temperature. In this case we have set $\chi = 0.83$ for both combining rules and T=285 K (P=2 MPa). The result was a flat potential energy pointing out a stable clathrate. This is shown in figure 6b. Increasing T upon 330 K does

not produce any sign of destabilization. Only the simulation performed at T=340 K leads to a destabilization. Thus, there is an important shift of the decomposition temperature towards larger values, implying a more stable clathrate structure by using the OPLS/AA for ethane molecules. Hence, explicit hydrogens do not supply any improvement. A structural change on ethane clathrates at T=340 K is far away from the temperature vicinity at which the system loses stability, according to the experiment.

The structural breakup from a crystal-like compound towards a liquid-like phase, can also be observed from the RDF's. In particular, we are showing in figure 7 the me–me RDF's for the SPC water model with standard combining rules, as a function of the temperature. The loss of stability of the ethane clathrate is obvious at T=330 K, in correspondence with strong changes of potential energy, number of hydrogen bonds, and water coordination numbers of ethane molecules. Figure 8 shows the RDF's estimated after including the χ parameter into the combining rules. Here we are showing 4 panels for the SCP water model. Panel a) shows the effect of χ when rescaling energy only for T=285 K. There it is observed that only a very low χ value is capable of destabilizing the clathrate. Panel b) shows the effect of temperature for a fitted $\chi = 0.035$. Here, it is shown that the system remains stable for T=250 K and turns clearly unstable for T=300 K. Panel c) shows the effect of varying χ when energy and size is affected for T=285 K. Panel d) shows the effect of temperature at a fixed parameter $\chi = 0.83$. All calculated data confirm the conditions at which the decomposition process takes place when the χ parameter was included in the cross interactions.

The PMF was also estimated for the ethane clathrates using the SPC water model at P=2 MPa. Figure 9a shows the PMF of CH3–CH3 association for two temperatures which are contained inside the vicinity of the transition line T=250 K and T=285 K. Using the standard Lorentz-Berthelot combining rules the crystalline compound is found in a stable phase for both temperatures. This property indicates that the proximity of two non-polar molecules is unfavourable at a stable thermodynamic state because water molecules are included inside the interstitial spaces. The crystalline compound became a destabilized system by modifying only the energetic parameter with $\chi = 0.035$ at T=285K. Figure 9b, shows the PMF for methyl-methyl groups for three different temperatures using the same value for $\chi = 0.035$ modifying just the energetic parameter as well. The system shows a significant change when varying the temperature from T=250 K to T=300 K. Figure 9c shows that the energetic barrier diminishes modifying the χ parameter at T=285 K. For this case both cross terms of the combining rules were modified at the same time. Figure 9d shows the PMF for ethane clathrates varying the temperature from T=250 K to T=300 K with $\chi = 0.85$ modifying the both Lorentz and Berthelot rules. Basically, the energetic barrier (Gibbs energy barrier ΔG) between two minima diminishes when the temperature is increased, in this case the solvent–separated configuration becomes the more relevant one. It means, the ethane molecules clustering is more favourable than otherwise. The diminishing of ΔG, which indi-

cates a destabilization of the crystalline compound, has already been observed on methane clathrates when the temperature is increased [57] and the same effect is observed when the pressure over the system is diminished keeping constant the temperature [61]. The ΔG was estimated at T=285 K for two cases. On one hand, using χ=0.035 and modifying just the energetic cross term. On the other hand, with χ=0.85 included on both combining rules. For the first case we obtained $0.33 \times 10^{20} J$ and for the second case was $0.23 \times 10^{20} J$. It seems to be that modifying just one cross term of the combining rules demands overcome a higher energetic barrier than that case when both cross terms were modified.

Finally, we show the MSD. This is another property which can be used to observe when the ethane clathrate is being destabilized. Dynamic and structural properties are, of course, linked. When the crystalline compound is simulated in a stable state, the guest molecule has limited displacements due to confinement. Thus as the stable state is being lost because of the temperature increment, the MSD dramatically increases, denoting the loss of the guest confinement. Figure 10 shows the MSD for ethane molecules over time using the SPC model for the water molecule at T=285 K and P=2 MPa. This is shown for three cases. By considering the energy rescaling of the pair potential with χ=0.035, with both, energy and distance rescaling (χ=0.83), and with no rescaling as a reference. The fluid-like behaviour of the MSD turns obvious for both modified interactions, whereas the reference case keeps a solid-like behaviour.

4 Concluding remarks

Molecular dynamics simulations for ethane clathrates on a NPT ensemble were performed. At low temperatures, all the water models used here reproduce very well the experimental RDFs for methyl–methyl groups as well as methyl–oxygen sites.
An exploratory study was carried out over the capabilities of different water models around the region of the phase-transition line (pressure – temperature). The estimation of the decomposition temperature was performed by monitoring different structural and dynamical properties. These are the ethane-water coordination number, the total number of hydrogen bonds, the potential energy, the potential of mean force and the mean square displacement. All these properties are strongly correlated and are appropriate to capture the decomposition of clathrates. The stable–unstable phase transition of crystalline compound was observed inside the temperature range of [320–440] K for all considered water models. They all are above the experimental result of 285 K, it means, none of the considered water models here is able to reproduce the experimental evidence using the standard combining rules. In this regard, we can mention that the SPC model showed the best performance since it produces the closer experimental decomposition temperature (320 K) whereas the TIP4P/ICE model

leads to the more stable clathrate (higher decomposition temperature 400 K). In fact, all the estimated properties show consistency among them. For instance, the TIP4P/ICE produces the same number of hydrogen-bonds and coordination number as SPC water model at T=250 K, however the first water model keeps these same numbers beyond T=400 K. Based on the above results, we can say the more stable is the crystalline compound, the more difficult is to reproduce the experimental temperature of transition by using the standard Lorentz-Berthelot rules.

The decomposition of the clathrate was not observed at the experimental temperature (285 K) when standard Lorentz-Berthelot combining rules were used. So, in order to approach the experimental decomposition temperature, a modification on the cross term of the combining rules was performed, by scaling only the interaction energy, on the one hand. And modifying both the interaction energy and distance at the same time, on the other. Thus, a scaling factor χ was introduced. The SPC water and NERD ethane models were used to test the inclusion of the χ factor. We have obtained $\chi = 0.035$ for the first case and $\chi = 0.85$ for the second one. We can mention that rescaling the intermolecular size is much more effective than rescaling energy alone. This means that the clathrate stability is sensitive to the size (hard core) of the guest molecule as well as the van der Waals contribution to the energy. In other words, the entropic contribution to the stability seems as important as the enthalpic one.

The TIP4P water model also was used to test the inclusion of the χ factor. The resulting factor was $\chi = 0.62$ which is lower than that for the SPC water model ($\chi = 0.85$). For this case it is necessary to use a lower value to weaken interaction between oxygen-methyl sites in order to reproduce the experimental transition temperature. In general, after including the factor χ in the cross terms, the interaction between water and guest becomes weaker and the effective diameter becomes smaller than the unmixed pure molecular species. In such a way, the stability of the crystalline compounds is not promoted since the weak interaction between two different type of molecules yields to the hydrophobic effect becomes less effective disrupting the hydrogen bonding attractions.

The OPLS-AA force field for ethane also was used into the simulations in order to analyse the effect of explicit hydrogen atoms, and as a result no improvement was observed. Actually, we found that the destabilization temperature (340 K) is higher than the experimental one, fixing $\chi = 0.83$. Finally, based on all above information, we found the SPC water and NERD ethane models are adequate to model the stable-unstable transition of the ethane clatrates. So, in a near future the effect of an external field over clathrates of ethane will be analysed using these molecule models with a modification on the cross term of the Lorentz-Berthelot rules.

Acknowledgement

GTG acknowledges CONACyT for supporting his M.Sc studies. DPL thanks to CONACyT for the support through the Cátedra CONACyT program. The authors thank the National Laboratory of High Performace (LANCAD) through the Laboratory of Parallel Supercomputing and Visualization (YOLTLA) at UAM-Iztapalapa for providing computational resource.

References

[1] R.K. McMullan and G.A. Jeffrey, J. Chem. Phys. **42** (1965) 2725

[2] T.C.W. Mak and R.K. McMullan, J. Chem. Phys. **42** (1965) 2732

[3] J.A. Ripmeester J.S. Tse C.I. Ratcliffe and B.M. Powell, Nature **325** (1987) 135

[4] E.D. Sloan, C.A. Koh, Clathrates Hydrates of Natural Gases, (CR Press, Taylor and Francis, Third Edition, 2008)

[5] Y. Jin, M. Kida, and J. Nagao, J. Phys. Chem. C, **117** (2013) 23469

[6] K. Shin, K.A. Udachin, I.L. Moudrakovski, D.M. Leek, S. Alavi, C.I. Ratcliffe, and J.A. Ripmeester, PNAS **110** (2013) 8437

[7] M.A. Kelland, T.M. Svartaas, J. Ovsthus and T. Namba, Annals N-Y Academic Sci. **912** (2006) 281

[8] J-W. Lee, S.-P. Kang, Chem. Eng. Trans. **32** (2013) 1921

[9] J. Jhaveri, J. Robinson, Can. J. Chem. Eng. **43** (1965) 75

[10] L.A. Báez, Crystal Nucleation and Growth. Molecular Dynamics Simulations of Hydrates Growth from water-gas mixtures. (Ph.D. Thesis Cornell University 1996).—

[11] N.J. English, J.M.D. MacElroy, Chemical Engineering Science **121** (2015) 133

[12] P.R. Bishnoi and V. Natarajan, Fluid Phase Equilib. **117** (1996) 168

[13] Y.F. Makogan, Hydrates of hydrocarbons, (PennWell Books Tulsa, Oklahoma, 1997)

[14] D.P. Luis, J. López-Lemus, M. Mayorga, Mol. Simul. **36** (2010) 461

[15] U. Marboeuf, N. Fray, O. Brissaud, B. Schmitt, D. Bockelee-Morvan and D. Gautier, J. Chem. Eng. Data, **57** (2012) 3408

[16] R.V. Belosludov, R.K. Zhdanov, O.S. Subbotin, H. Mizuseki, M. Souissi, Y. Kawazoe and V.R. Belosludov, Mol. Sim. **38** (2012) 773

[17] K. Tumba, P. Naidoo, A.H. Mohammadi, D. Richon, and D. Ramjugernath, J. Chem. Eng. Data, **58** (2013) 896

[18] K. Morita, S. Nakano, K. Ohgaki, Fluid Phase Equlib. **169** (2000) 167

[19] M. Naseh, V. Mohebbi, and R.M. Behbahani, J. Chem. and Eng. Data **59** (2014) 3710

[20] H. Tanaka, J. Chem. Phys. **101** (1994) 10833

[21] H.J.C. Berendsen, J.P.M. Postma, W.F. van Gunsteren, and J. Hermans, In Intermolecular Forces, edited by B. Pullman (Reidel, Dordrecht, 1981), p. 331.

[22] H.J.C. Berendsen, J.R. Grigera, and T.P. Straatsma, J. Phys. Chem. **91** (1987) 6269

[23] W.L. Jorgensen and J.D. Madura, Mol. Phys. **56** (1985) 1381

[24] J.L.F. Abascal and C. Vega, J. Chem. Phys. **123** (2005) 234505

[25] J.L.F. Abascal, E. Sanz, R.G. Fernández, and C. Vega, J. Chem. Phys. **122** (2005) 234511

[26] J. Alejandre, G.A. Chapela, H. Saint-Martin and N. Mendoza, Phys. Chem. Chem. Phys. **13** (2011) 19728

[27] M.W. Mahoney and W.L. Jorgensen, J. Chem. Phys. **112** (2000) 8910

[28] S.K. Nath, F.A. Escobedo, and J.J. de Pablo, J. Chem. Phys. **108** (1998) 9905

[29] W.L. Jorgensen, D.S. Maxwell and J. Tirado-Rives, J. Am. Chem. Soc. **118** (1996) 11225

[30] H.A. Lorentz, Ann. Phys. **12** (1881) 127

[31] D.C. Berthelot, Sur le Melange des Gaz, Compt. Rend. **126** (1898) 1703

[32] J. Vrabec, J. Stoll and H. Hasse, Mol. Simul. **31** (2005) 215

[33] A.J. Haslam, A. Galindo, G. Jackson, Fluid Phase Equilib. **266** (2008) 105

[34] J. Delhommelle and P. Millie, Molec. Phys., **99** (2001) 619

[35] E. Díaz-Herrera, G. Ramírez-Santiago and J.A. Moreno-Razo, J. Chem. Phys. **123** (2005) 184507

[36] H. Doherty, A. Galindo, C. Vega, E. Sanz, J. Phys. Chem. B, **111** (2007) 8993

[37] M. Lasich, A.H. Mohammadi, K. Bolton, J. Vrabec, D. Ramjugernath, Fluid Phase Equilib. **381** (2014) 108

[38] M.M. Conde and C. Vega, J. Chem. Phys. **133**m (2010) 064507

[39] I.N. Tsimpanogiannis, N.I. Diamantonis, I.G. Economou, N.I. Papadimitriou, A.K. Stubos, Chem. Eng, Research and design **92** (2014) 2992

[40] N.I. Papadimitriou, I.N. Tsimpanogiannis, I.G. Economou, A.K. Stubos, Mol. Phys. **112** (2014) 2258

[41] B. Hess, C. Kutzner, D. van der Spoel, E. Lindahl, J. Chem. Theory Comput. **4** (2008) 435

[42] E. Lindahl, B. Hess, D. van der Spoel, J. Mol. Mod. **7** (2001) 306

[43] H.J.C. Berendsen, D. van der Spoel, R. van Drunen, Comp. Phys. Comm. **91** (1995) 43

[44] H.J.C. Berendsen, J.P.M. Postma, W.F. van Gunsteren, J. Hermans, Interaction Models for Water in Relation to Protein Hydration, in Intermolecular Forces, B. Pullman, ed., D. Reidel Publishing Company, Dordrecht, (1981) 331

[45] U. Essmann, L. Perera, M.L. Berkowitz, T. Darden, H. Lee, L.G.J. Pedersen, J. Chem. Phys. **103** (1995) 8577

[46] B. Hess, H. Bekker, H.J.C. Berendsen, J.G.E.M. Fraaije, J. Comput. Chem. **18** (1997) 1463

[47] H.J.C. Berendsen, J.P.M. Postma, W.F. van Gunsteren, A. DiNola, J.R. Haak, J. Chem. Phys. **81** (1984) 3684

[48] G.J. Martyna, M.L. Klein, M.E. Tuckerman, J. Chem. Phys. **97** (1992) 2635

[49] M. Parrinello, A. Rahman, J. Appl. Phys. **52** (1981) 7182

[50] R.K. McMullan and G.A. Jeffrey, J. Chem. Phys. **42** (1965) 2725

[51] R.T. Morrison, R.N. Boyd, Organic Chemistry, (Sixth Edition, Prentice-Hall, Inc. 1992)

[52] J.R. Couper, W.R. Penney, J.R. Fair, S.M. Walas, Chemical Process Equipment revised: Selection and Design, (Second Edition, Elsevier Inc. 2010)

[53] J.D. Bernal and R.H. Fowler, J. Chem. Phys. **1** (1933) 515

[54] D. Chandler, Introduction to Modern Statistical Mechanics, Oxford University Press, New York, 1987.

[55] A. Luzar, D. Chandler, Nature **379** (1996) 55

[56] M.P. Allen and D. Tildesley, Computer Simulation of Liquids, Clarendon Press, Oxford, 1987.

[57] D.P. Luis, J. López-Lemus, M. Mayorga and L. Romero-Salazar, Mol. Simul. **36** (2010) 35

[58] R.L. Mancera, and A.D. Buckingham, J. Phys. Chem. **99** (1995) 14632

[59] A.A. Chialvo, M. Houssa, and P.T. Cummings, J. Phys. Chem. B **106** (2002) 442

[60] H. Docherty, A. Galindo, C. Vega, E. Sanz, J. Chem. Phys. **125** (2006) 074510

[61] G. Hummer, S. Garde, A.E. García, M.E. Paulaitis, and L.R. Pratt, Proc. Natl. Acad. Sci. **95** (1998) 1552

Figure Caption

Figure 1, CH_3–CH_3 RDF's at T=200 K and P=2 MPa. Different water models were used. Open diamonds TIP5P, crosses TIP4P/ICE, asterisk TIP4P/2005, open triangles TIP4Q, open squares TIP4P, open circles SPC/E and plus symbols for SPC model.

Figure 2, CH_3–O RDF's at T=200 K and P=2 MPa. Different water models were used. The symbols have the same meaning as figure 1.

Figure 3, Snapshot of the ethane clathrates using SPC water model at T=250 K and P=2 MPa.

Figure 4, coordination number at P=2 MPa as a function of temperature. a) for $\chi = 1$ and b) varying the χ parameter. The symbols have the same meaning as figure 1.

Figure 5, hydrogen-bonds as a function of temperature. Different water models were used. a) for $\chi = 1$ and b) varying the χ parameter. The description for each water model is contained in the inset.

Figure 6, potential energy at P=2 MPa. a) the lower curve corresponds to the results derived at T=285 K, the upper curve was calculated at T=330 K, using standard Lorentz-Berthelot combining rules in both cases. The curves which are between the previous ones were calculated at T=285 K. The continues line was derived by using the $\chi = 0.83$ and the curve with up-triangles correspond to results from $\chi = 0.035$. b) The OPLS/AA model for ethane was used with $\chi = 0.083$, the curves, from bottom to top, correspond to results derived at T=285 K (open squares), T=330 K (open diamond) and T=340 K (open down-triangles), respectively.

Figure 7, CH_3–CH_3 RDF's as a function of temperature using standard Lorentz-Berthelot rules at P=2 MPa. The description of the curves is contained in the inset.

Figure 8, CH_3–CH_3 RDF's at P=2 MPa using the SPC water model. As a first approximation the combining rule for ϵ_{ij} was modified with the χ parameter, a) fitting the temperature and varying the parameter χ. b) fitting the χ parameter and varying the temperature. The second approximation both combining rules were modified, c) for T=285 K and varying the χ parameter and d) fitting the $\chi = 0.83$ parameter but varying the temperature. See the inset for the meaning of the symbols.

Figure 9, PMF at P=2 MPa. Show the curves derived by modifying just the energetic parameter from the cross term. a) for a fixed temperature T=285 K and different values for

χ parameter and b) for $\chi = 0.035$ and several temperatures. Furthermore some curves are shown including χ parameter on both Lorentz-Berthelot combining rules. c) for T=285 K varying the χ parameter, and d) for $\chi = 0.83$ parameter and three temperatures.

Figure 10, MSD at T=285 K and P=2 MPa. The open up-triangles correspond to the results estimated with $\chi = 1$. The open circles are the results calculated with $\chi = 0.035$, where just the ϵ_{ij} parameter was modified. The open squares were obtained using $\chi = 0.83$ when both the arithmetic and geometric combining rules were modified at the same time.

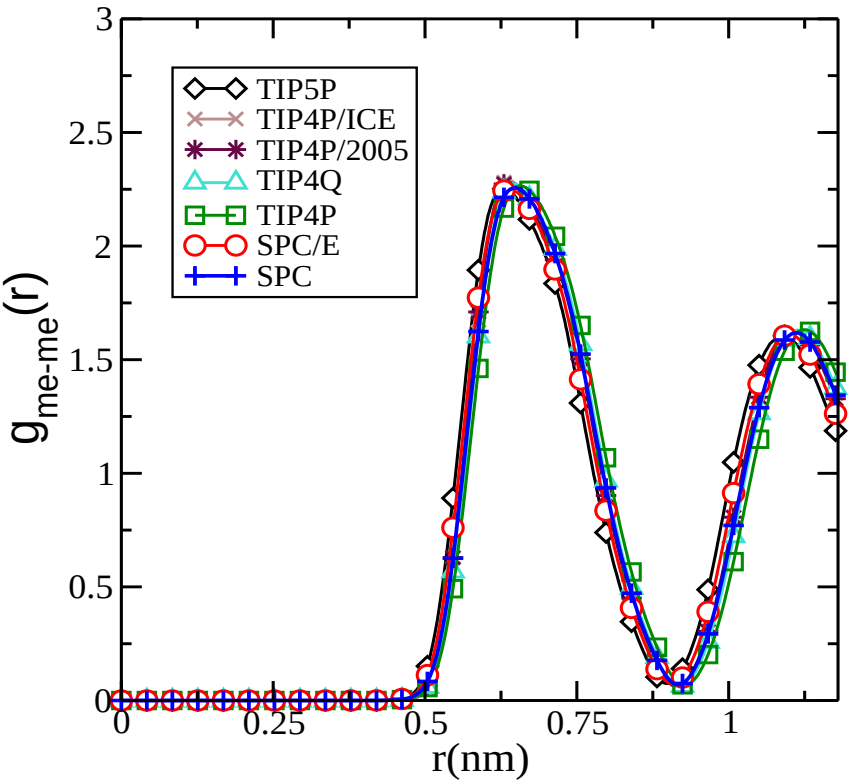

Figure 1, CH_3–CH_3 RDF's at T=200 K and P=2 MPa. Different water models were used. Open diamonds TIP5P, crosses TIP4P/ICE, asterisk TIP4P/2005, open triangles TIP4Q, open squares TIP4P, open circles SPC/E and plus symbols for SPC model.

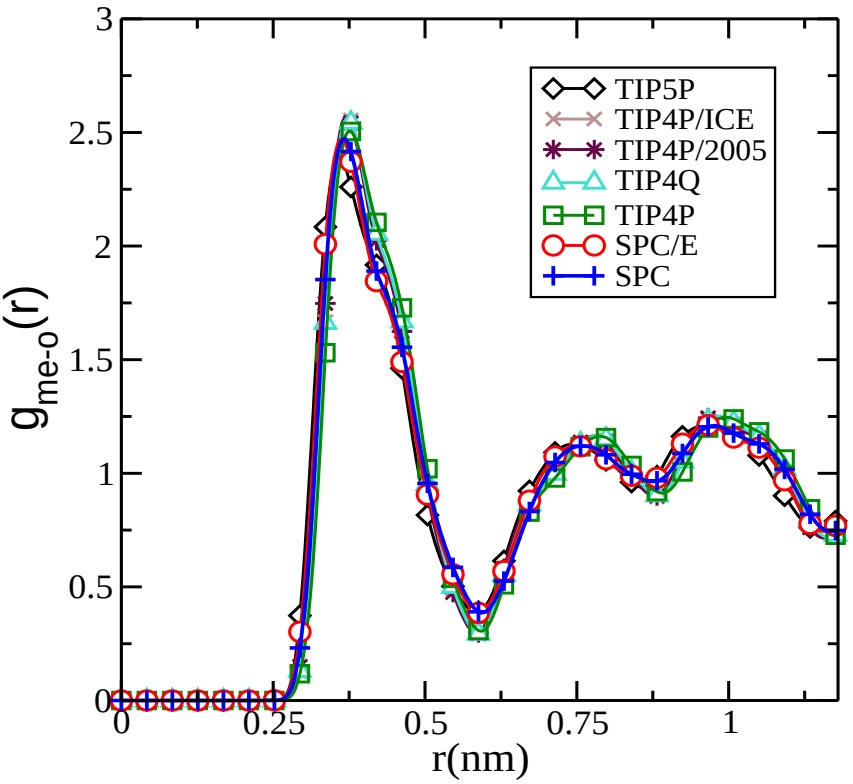

Figure 2, CH_3–O RDF's at T=200 K and P=2 MPa. Different water models were used. The symbols have the same meaning as figure 1.

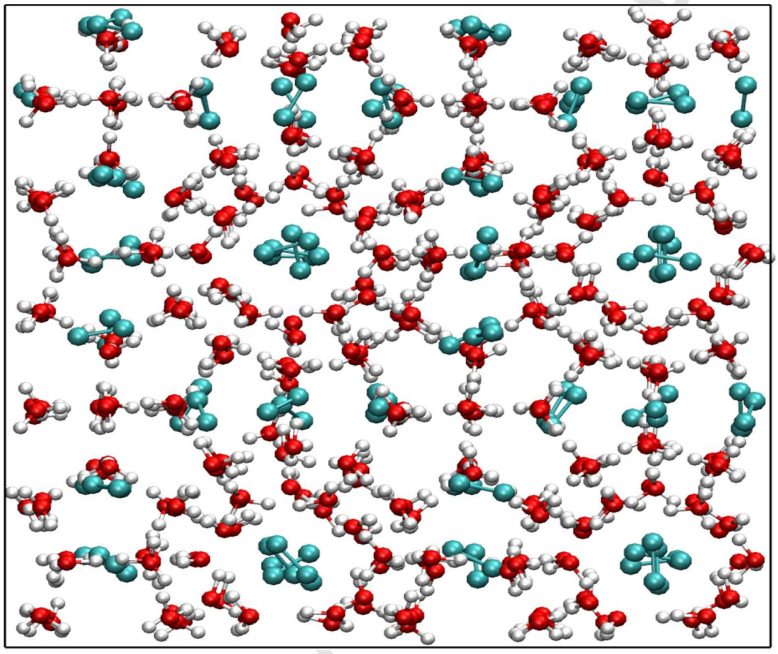

Figure 3, Snapshot of the ethane clathrates using SPC water model at T=250 K and P=2 MPa.

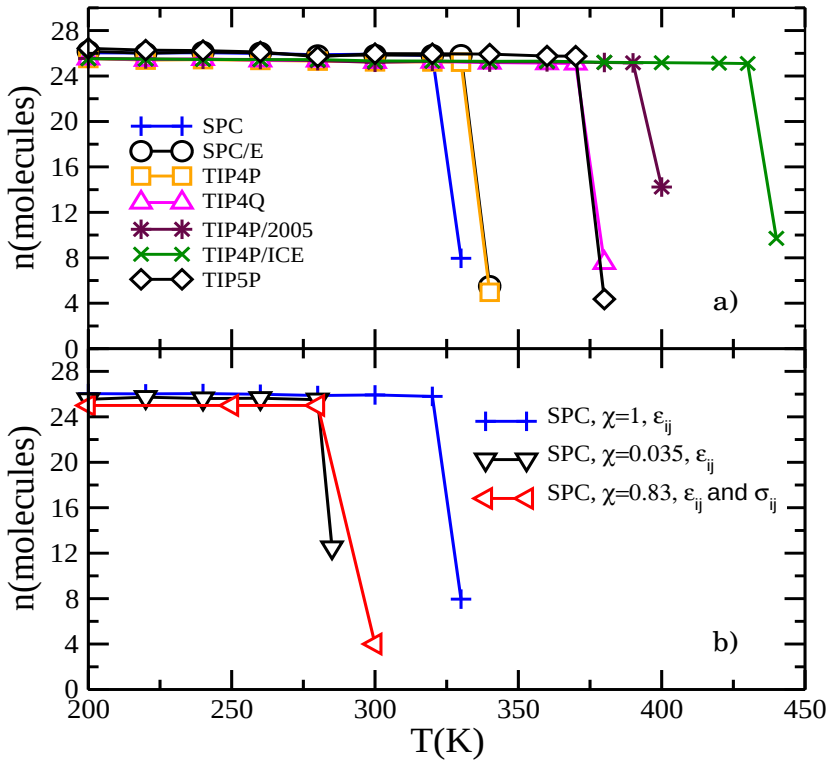

Figure 4, coordination number at P=2 MPa as a function of temperature. a) for $\chi = 1$ and b) varying the χ parameter. The symbols have the same meaning as figure 1.

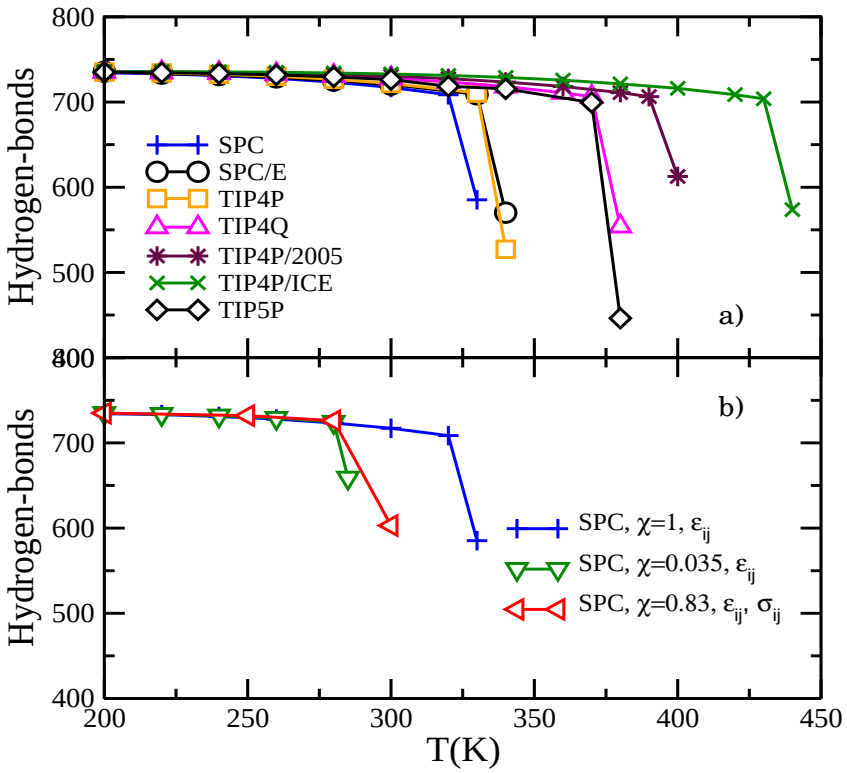

Figure 5, hydrogen-bonds as a function of temperature. Different water models were used. a) for $\chi = 1$ and b) varying the χ parameter. The description for each water model is contained in the inset.

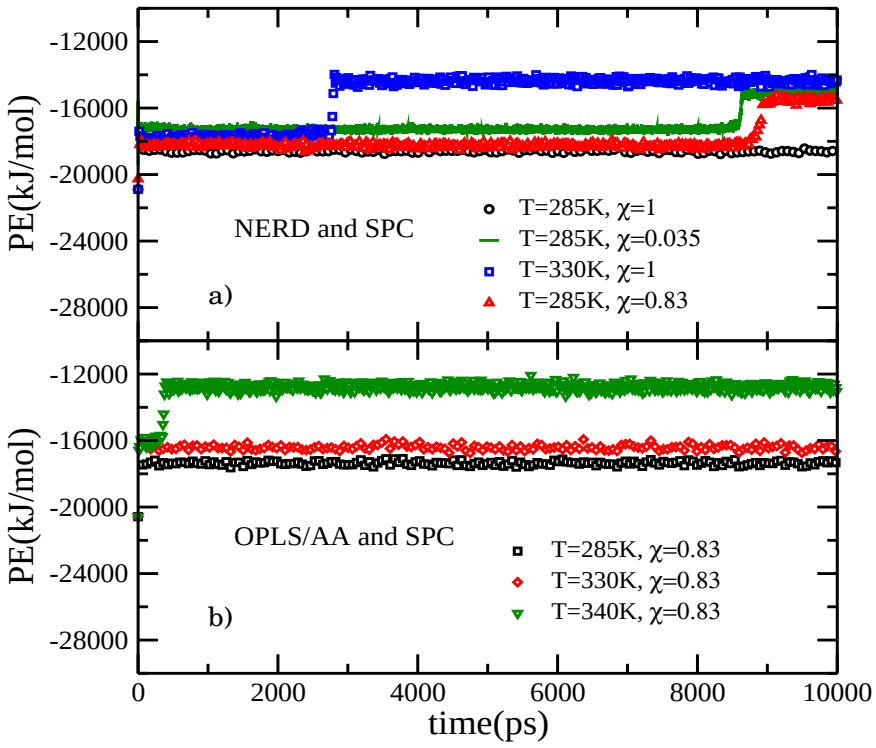

Figure 6, potential energy at P=2 MPa. a) the lower curve corresponds to the results derived at T=285 K, the upper curve was calculated at T=330 K, using standard Lorentz-Berthelot combining rules in both cases. The curves which are between the previous ones were calculated at T=285 K. The continues line was derived by using the $\chi = 0.83$ and the curve with up-triangles correspond to results from $\chi = 0.035$. b) The OPLS/AA model for ethane was used with $\chi = 0.083$, the curves, from bottom to top, correspond to results derived at T=285 K (open squares), T=330 K (open diamond) and T=340 K (open down-triangles), respectively.

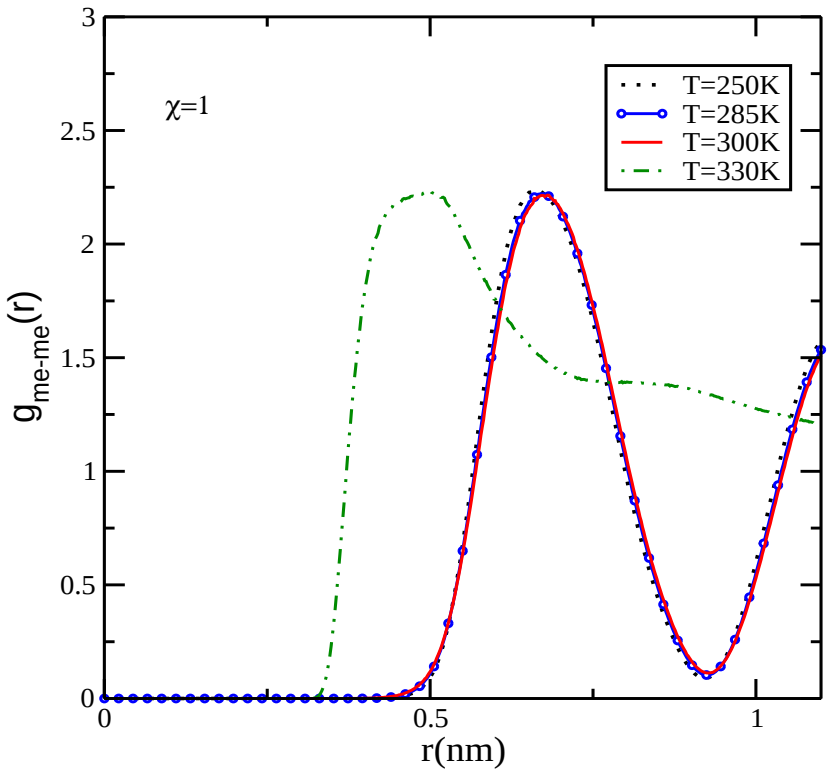

Figure 7, CH_3–CH_3 RDF's as a function of temperature using standard Lorentz-Berthelot rules at P=2 MPa. The description of the curves is contained in the inset.

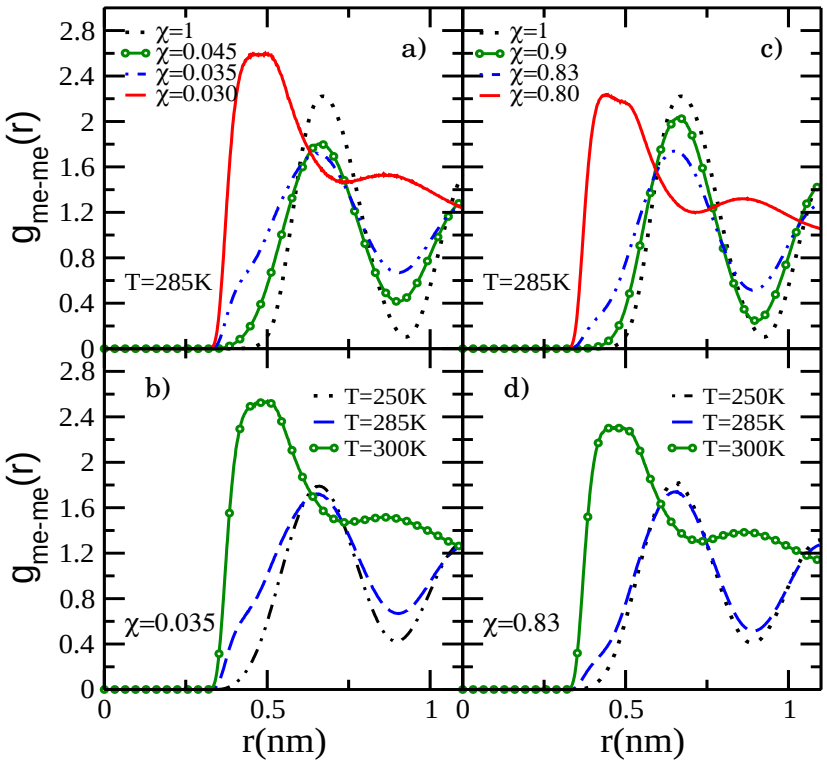

Figure 8, CH_3–CH_3 RDF's at P=2 MPa using the SPC water model. As a first approximation the combining rule for ϵ_{ij} was modified with the χ parameter, a) fitting the temperature and varying the parameter χ. b) fitting the χ parameter and varying the temperature. The second approximation both combining rules were modified, c) for T=285 K and varying the χ parameter and d) fitting the $\chi = 0.83$ parameter but varying the temperature. See the inset for the meaning of the symbols.

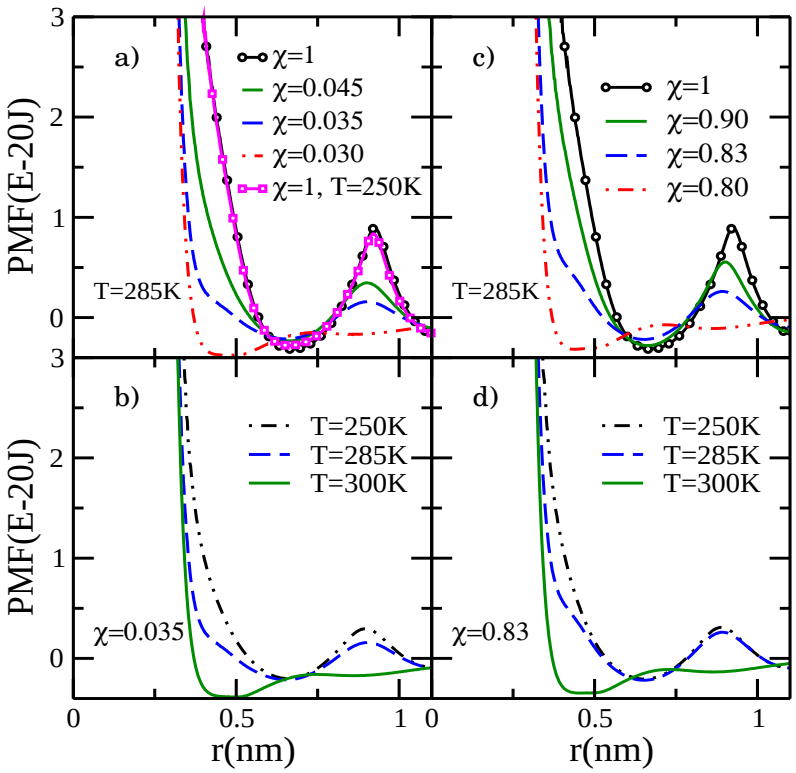

Figure 9, PMF at P=2 MPa. Show the curves derived by modifying just the energetic parameter from the cross term. a) for a fixed temperature T=285 K and different values for χ parameter and b) for $\chi = 0.035$ and several temperatures. Furthermore some curves are shown including χ parameter on both Lorentz-Berthelot combining rules. c) for T=285 K varying the χ parameter, and d) for $\chi = 0.83$ parameter and three temperatures.

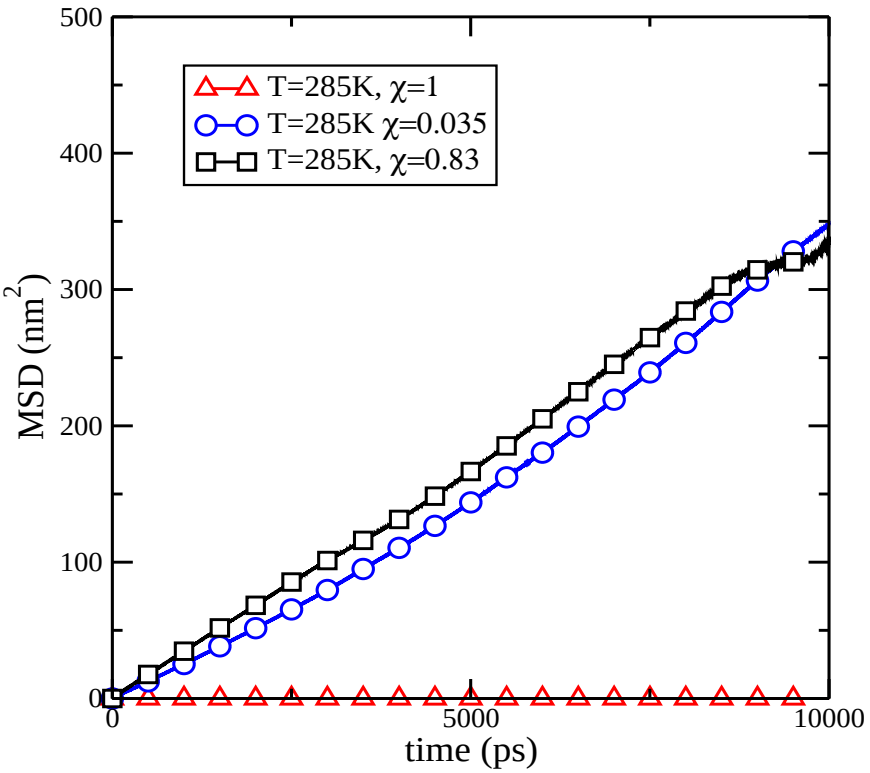

Figure 10, MSD at T=285 K and P=2 MPa. The open up-triangles correspond to the results estimated with $\chi = 1$. The open circles are the results calculated with $\chi = 0.035$, where just the ϵ_{ij} parameter was modified. The open squares were obtained using $\chi = 0.83$ when both the arithmetic and geometric combining rules were modified at the same time.